# Nonstationary Random Pulses Representation of Ground Roughness for Taxiing Aircraft

Robert P. Chen*
*The Garrett Corporation, Los Angeles, Calif.*
and
Michael C. Bernard†
*Georgia Institute of Technology, Atlanta, Ga.*

**This paper presents a general method of describing both nonstationary and stationary roughness experienced by an aircraft taxiing on ground. The generalized roughness spectrum is shown to be in agreement with previously published results. It also reduces to the similar form of the one-runway-one-speed case presently employed by the aircraft industry. These procedures, however, assume that the input spectra of either the velocity components of atmospheric turbulence or the runway roughness are stationary instead of nonstationary as is actually the case. Recently, studies were made on nonstationary flight vehicle gust response and rotor blade vibrations. However, since no attempt was made to treat the taxiing problem accordingly, this work was undertaken.**

## Introduction

THE dynamic response of airplanes to random loading has been studied by use of power spectral density methods for some time. Liepmann[1] and Press and Mazelsky[2] applied the methods to buffeting problems and gust loads, respectively, as early as 1952-53. Fung[3] presented the first example in the aeronautical field to treat the forcing function as a nonstationary process. Recently, there have been a number of papers on nonstationary gust response of flight vehicles,[4] rotor blade vibrations,[5] and responses of cantilever beams.[6]

Pioneering works in runway roughness studies by power spectral methods may be found in the publications of Walls, etc.,[7] and Houbolt, etc.[8] Many studies on the subject have appeared since the late 1950's and early 1960's. Most of them[9] have been either purely experimental in nature,[10,11] or have concentrated on the development of roughness criteria or the quantitative evaluation of roughness spectra from various sites. Some investigators[12,13] have suggested treating the airplane taxiing problem as a deterministic process. They have obtained reliable response results for particular segments of certain given runways. In order to account for the chance encounter of different runways with varying roughnesses, it is only reasonable to approach the problem in a probabilistic way, using power spectral techniques developed from random processes.

An imminent need in the airplane taxiing problem, therefore, is the development of a methodology that will account for the different levels of measured roughnesses in their existing format: i.e., power spectral densities or profile elevations together with a rational probability distribution for the arrival times of taxi events for the airplanes from post utilization records or prospective requirements. This information will require the treatment of the roughness inputs as a piece-wise stationary process with the current stationary one-runway-one-taxi-speed analysis and any deterministic roughness approaches included as special cases. More precisely, the development of such a composite roughness input may be described briefly as a sequence of nonstationary pulses, with random strength and shape for each constituent pulse obtained from the specific runway where the taxi event took place. It is interesting to find that Lin[14,15] has published a series of papers on nonstationary shot noise, the last of which may be modified to describe exactly the process needed to specify the composite roughness input.

Received July 30, 1975; revision received May 28, 1976.
Index categories: Aircraft Flight Operations; Aircraft Landing Dynamics; Aircraft Vibration.

*Engineer, AiResearch Manufacturing Division.
†Associate Professor, Engineering Science and Mechanics.

## Philosophical Background

The methodology of representing a probable set of runway roughnesses, ranging from well-maintained airports to unprepared front-line airstrips as nonstationary random pulses may be understood by considering the actual aircraft operations and their omnipresent environmental disturbances. The philosophy is exemplified by a typical time history of the wing bending moment of a conventional airplane. It is further stipulated that the atmospheric gust responses contribute to the total fatigue damage of the airframe only in a fashion described as G-A-G (ground-air-ground) cycles; hence, it is permissible to assume all the time periods other than ground operations quiescent. (Houbolt[16] employed the same argument for gust response studies.)

With the removal of the airborne disturbances and the aerodynamic or velocity sensitive phases of ground operations – i. e., atmospheric gust response, landing impact, high/low speed take-off, and landing roll-out – the response time history is reduced to a sequence of time-history segments with the elapsed air times preserved between the neighboring constant speed taxis and the previously cited disturbances replaced by undisturbed time segments of corresponding lengths. The simplicity of the resulting sequential constant speed taxi response realization is shown in Fig. 1.

The excitation process that generates such a response time history can be deduced from the same argument. If the geographical elevations of the runway/taxiway sites and their long wavelength unevenness from the underlying topological structures of the subsoils are removed, the roughness profiles that correspond to the sample response realization of Fig. 2 may be obtained by substituting the segmented response time histories by the respective roughness measured from their individual mean profiles. A representative sequence of roughnesses corresponding to the response time history of Fig. 1 is shown in Fig. 2. It must be remembered that in converting the runway/taxiway horizontal distances used for each constituent roughness profile, an arbitrary contracting or expanding scale factor was employed, which is equivalent to the reciprocal of the particular constant taxi speed of a given

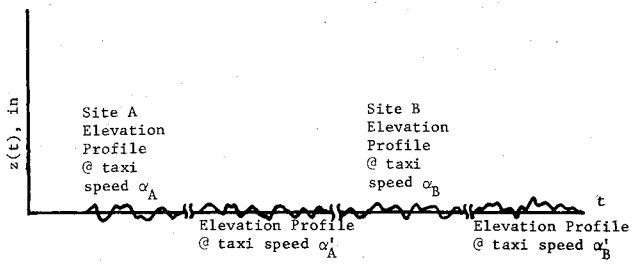


**Fig. 1 Typical aircraft wing bending moment record.**

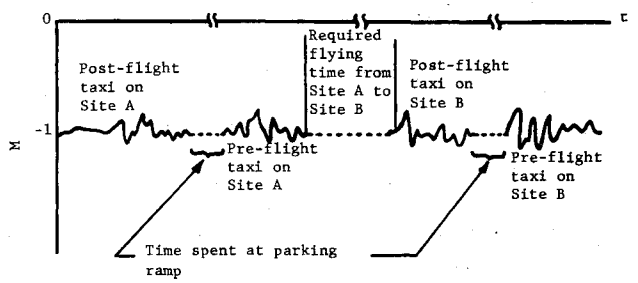


**Fig. 2 Sequence of taxi events.**

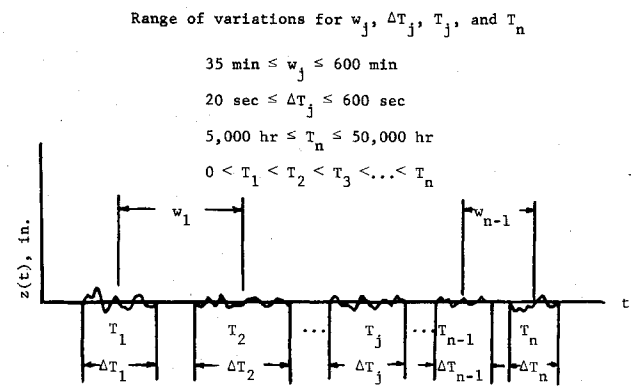


**Fig. 3 Ground roughness time history corresponding to the above taxi events.**

segment. This linear transformation can be expressed as

$$D_i = \int_0^{\Delta T_i} v(t)\,dt = V_i \Delta T_i \tag{1}$$

where $V_i$ is a random variable within a given range ($V_i \geq 0$), and $D_i$ a random variable denoting the horizontal distance traveled within a time segment $\Delta T_i$ for the constant speed taxis.

In anticipation of using the random pulse representation, and in awareness of the complex notation required, it is advantageous to relax the restriction on the randomness of $V_i$, although it has been observed to be related inversely to ground roughness in normal operations. From an engineering viewpoint, the ranges of $V_i$ and $D_i$ are fairly limited for existing airplanes and airports. It is conservative to say that $V_i$ is in the interval (10kts, 100kts) and $D_i$ is in the interval (2,000 ft, 10,000 ft). The most adverse combination of these values gives the segmented taxi time $\Delta T_i$ in the interval (20 sec, 600 sec). Bearing in mind that the service life of the present generation of airplanes is of the order of 5,000 hr for a fighter and 50,000 hr for a commercial airliner, and allowing the shortest service life (5,000 hr) to be the total time of a given realization, it is found that the longest taxi time (600 sec) per flight is a mere 1/30,000 of the total time. It is therefore insignificant to consider the contracting or expanding of a particular constant speed taxi segment. It is also found that the flying time $w_i$ for a short-haul flight and an intercontinental flight are 35 min and 10 hr, respectively. Thus, the criterion for the spacing of the composite roughness time history similar to that of Fig. 2 is established as the flight time. A typical realization experienced by a given aircraft with the composite roughness of the taxi segments stretched is illustrated with the range of the spacings, i. e., the flight times, shown in Fig. 3.

## Generation of Roughness Pulses Sequences

The task of obtaining the composite roughness pulses will be complete once the vast amount of existing power spectral density (PSD) data on runway/taxiway roughness, together with the utilization and mission profile of a given aircraft and/or types of aircraft, are furnished to the airframe manufacturer for the analysis of the design of a prospective aircraft. The same information may also be derived from a systematic compilation of existing fleet operations by monitoring closely the daily utilization of each aircraft within the fleet of different types of airplanes for an extended observation period. The procedure will be described fully, using the schematic diagram of Fig. 4 for an ensemble of airplanes and/or types of airplanes operating on assorted roughnesses for a finite time period. Each realization is generated in the same fashion as that of Fig. 3, with the exception that each roughness is contracted to a point on the time axis, the roughness strength is represented by the height of each stroke, and the superscript denotes a member aircraft in a fleet or a given type of aircraft in existence which resembles the new aircraft in operational characteristics.

From the preceding paragraph, it is understood that the power spectral densities of the roughness of the probable taxi sites are given a priori. It is further postulated that all the roughness power spectral densities are expressed in spatial frequencies, that is, $\Omega = \omega / V_{\text{TAXI}}$. Hence, the Wiener-Khintchine relations for a given runway/taxiway become

$$\Phi_{zz}(\Omega) = \frac{1}{2\pi} \int_{-\infty}^{\infty} R_{zz}(\lambda) e^{-j\Omega\lambda} d\lambda \tag{2a}$$

$$R_{zz}(\lambda) = \int_{-\infty}^{\infty} \Phi_{zz}(\Omega) e^{j\Omega\lambda} d\Omega \tag{2b}$$

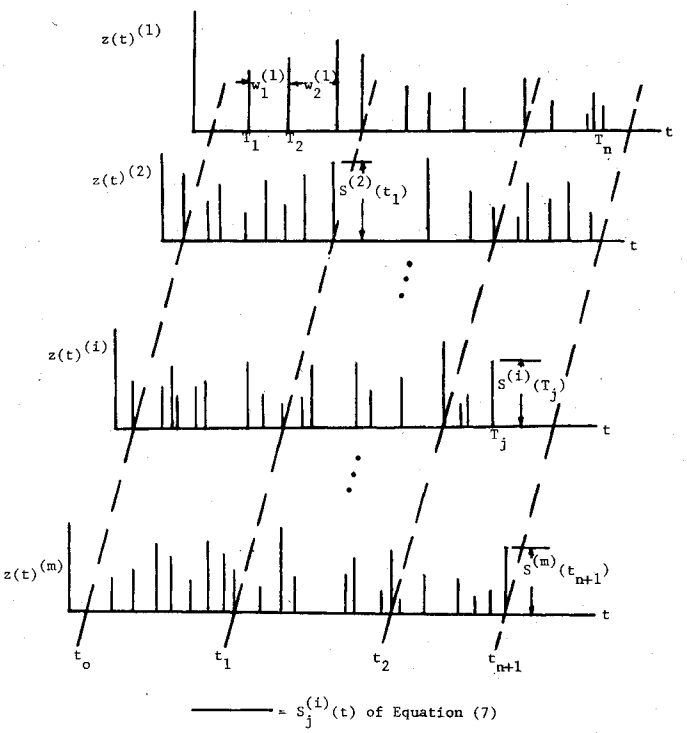


**Fig. 4 Typical composite roughness with flying time spacing.**

where $\lambda$ is the lag distance and may be expressed as

$$\lambda = V_{TAXI} \cdot \tau \tag{3}$$

With $V_{TAXI}$ equal to a given constant, and $\tau$ being the dummy variable for the lag time of the temporal power spectral density, Eqs. (2a) and (2b) can be written as

$$\Phi_{zz}(\omega) = \frac{1}{2\pi} \int_{-\infty}^{\infty} R_{zz}(\tau) e^{-j\omega\tau} d\tau \tag{4a}$$

$$R_{zz}(\tau) = \int_{-\infty}^{\infty} \Phi_{zz}(\omega) e^{j\omega\tau} d\omega \tag{4b}$$

A sample roughness spectrum and its autocorrelation function is shown in Fig. 5.

Most of the roughness autocorrelations can be approximated by

$$R_{zz}(\lambda) = \sigma_{zz}^2 e^{-\beta|\lambda|} \qquad \beta > 0 \tag{5}$$

where $\beta$ is a given shaping factor, and $\sigma_{zz}^2$ is the roughness variance of the given runway. From Eqs. (3) and (5), it is clear that for a given runway at a given taxi speed $\alpha$

$$R_{zz}(\lambda) = \sigma_{zz}^2 e^{-\beta|\lambda|} = \sigma_{zz}^2 e^{-\alpha\beta|\tau|} \tag{6}$$

At this stage, two quantities will be defined to fulfill the formulation of the composite roughness description of a given realization. First, let

$$S_j^{(i)}(t) = \sigma_{zz}^{(i)}(T_j) e^{-\gamma_j^{(i)}|t-T_j|} \tag{7}$$

where $\sigma_{zz}^{(i)}(T_j)$ is the roughness strength at time $T_j$ from the $i$th record, $e^{-\gamma_j^{(i)}|t-T_j|}$ is the pulse shape at time $T_j$ from the $i$th record, and

$$\gamma_j^{(i)} = \alpha_j^{(i)} \beta_j^{(i)} \qquad t_o \le T_j \le t_{n+1},\ j = 1, 2, 3, \ldots, n$$

$S_j^{(i)}(t)$ equals the shaped roughness pulse for a time interval $\Delta T_j$. Secondly, let $n$ equal the arrival rate of taxi events. It may be represented by the following integral

$$n = \int_{t_j}^{t_k} n(\tau),\ t_o \le t_j < t_k \le t_{n+1} \tag{8}$$

where $n$ is the number of taxi events in the time interval $(t_j, t_k)$. It should be noted that $t_o$ and $t_{n+1}$ are chosen without any loss of generality as the first and last taxi time of an ensemble (see Fig. 4). If zero roughness strength is permitted for the null event in which no taxi operations have been encountered, then $t_o$ and $t_{n+1}$ can take on values of $(-\infty)$ and $(+\infty)$, respectively.

## Sources of Nonstationarity

With the roughness pulse and the arrival rate of taxi events thus defined, it is clear that a given composite roughness record is a truly nonstationary phenomenon. The nonstationarity arises from the time-dependent expressions of Eqs. (7) and (8) for the roughness pulse and the arrival rate of taxi events, respectively.

From the unpredictable nature of $w_j$, the flying time, it is convenient to assume that the uncorrelated arrival rate of taxi events $n$ is governed by a nonhomogeneous Poisson distribution given by Laning and Battin[17] as

$$P_{\{N\}}(n, t) = \frac{1}{n!} \left[ \int_{t_o}^{t} n(\tau) d\tau \right]^n \exp\left[ \int_{t_o}^{t} n(\tau) d\tau \right]$$

where $\{N\} = n$, the number of arrivals of Eq. (8). The nonstationarity of the roughness pulse is studied with different goals of analyses in mind. The approaches used for the individual categories are delineated in the following subsections.

### Design Criteria Development for New Aircraft

The requirement for this analysis pertains to the acquisition of a representative composite roughness record which may approximately encompass the totality of all possible taxi site roughnesses accessible to all types of airplanes whose operational characteristics are being incorporated in the new design. The method of assessing such an averaged record is equivalent to calculating the instantaneous ensemble average over the finite collection of composite roughnesses of available types of airplanes. Let $\{Z^{(i)}(t)\}$, $i = 1, 2, 3, \ldots m$ be the composite roughness records of $m$ types of existing aircraft as shown in Fig. 4. It is now asserted that $m$ is fairly large such that the mathematical expectation of the roughness pulse may be calculated as

$$\begin{aligned} E[S(t)] &= \lim_{m\to\infty} \frac{1}{m} \int_o^{\infty} \sum_{i=1}^{m} sp_S^{(i)}(s, t)\, ds \\ &= \lim_{m\to\infty} \frac{1}{m} \sum_{i=1}^{m} E[S^{(i)}(t)] \quad \text{for } i = 1, 2, \ldots, m \\ &\qquad \text{and } t_o \le t \le t_{n+1} \end{aligned} \tag{9}$$

where $p_S^{(i)}(s, t)$ is the time-dependent probability density function for the magnitude of the roughness pulse for aircraft type $i$ and it has been assumed that the operations of integration and summation can be interchanged.

### Fatigue Life Evaluation for Fleet Operations

The main feature for this analysis is that the ensemble of composite roughness records is taken from one type of aircraft and the mathematical expectation can be deduced from Eq. (9) in the following manner

$$E[S(t)] = \int_o^{\infty} sp_S(s, t)\, ds \tag{10}$$

where the superscript $(i)$ is dropped from the probability density function because the type is unique. It is interesting to note that both of the expected roughness strength functions as expressed in Eqs. (9) and (10) are still time-dependent and thus nonstationary.

## Determination of Pulse Shapes

Figure 6 shows a typical composite roughness record for the design criteria development analysis. A typical record for the fleet fatigue evalution analysis is obtained simply by using the appropriate averages in place of $\bar{\sigma}_{zz}$ and $\bar{\gamma}_j$. It is understood from Eq. (9) that to obtain the expected roughness pulse $E[S(t)]$ at a given time $t = T_j$, the calculation involves an averaging over the appropriate types. Further, Eq. (7) shows that the instantaneous magnitude of the roughness pulse at time $t$, $s(t)$ is composed of two parts, $\sigma_{zz}(T_j)$ and $e^{-\sigma_j|t-T_j|}$.

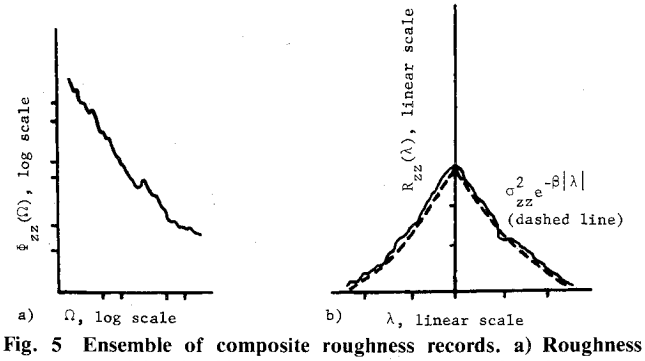


**Fig. 5 Ensemble of composite roughness records. a) Roughness power spectral density. b) Roughness autocorrelation function.**

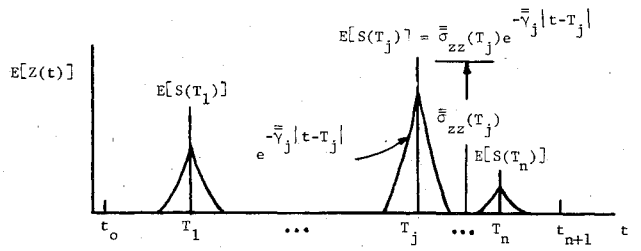


**Fig. 6 Typical composite roughness record for design criteria development.**

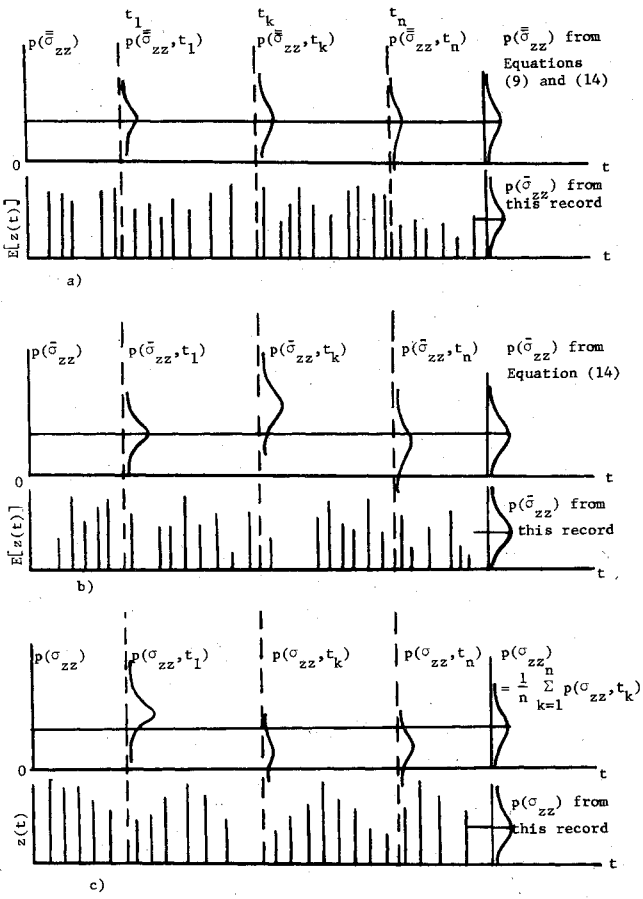


**Fig. 7 Typical composite roughness record for design criteria development. a) Design criteria development. b) Fleet fatigue life evaluation. c) One-aircraft ground loads survey.**

The former is the $\sigma_{zz}$ value of the roughness strength of a given runway for the taxi event at time $T_j$, while the latter is a taxi speed-sensitive pulse shape, if one recalls that $\gamma_j = \alpha_j \beta_j / 2$, and $\alpha_j$ is the given taxi speed at time $T_j$. Hence, the abbreviated probability density function $p_S(s, t)$ may be expressed in full as

$$p_S(s, t) = p(\sigma_{zz}, \gamma, T_j) \quad \text{for } t = T_j \tag{11}$$

If this bivariate density function is used in Eq. (10), the expected roughness at time $T_j$ will be

$$E[S(T_j)] = \int\int_0^\infty \sigma_{zz}(T_j) e^{-\sigma |t-T_j|} p(\sigma_{zz}, \sigma, T_j) d\sigma_{zz} d\sigma \tag{12a}$$

Here $\sigma_{zz}^2(T_j) = R_{zz_{T_j}}(0)$, where $R_{zz_{T_j}}(0)$ is the area under the roughness power spectral density of the runway to be traversed at time $T_j$. $R_{zz_{T_j}}(0)$ is a quantity independent of taxi speed, as shown by setting $\tau = 0$ in Eq. (3) to obtain $\lambda = 0$ for

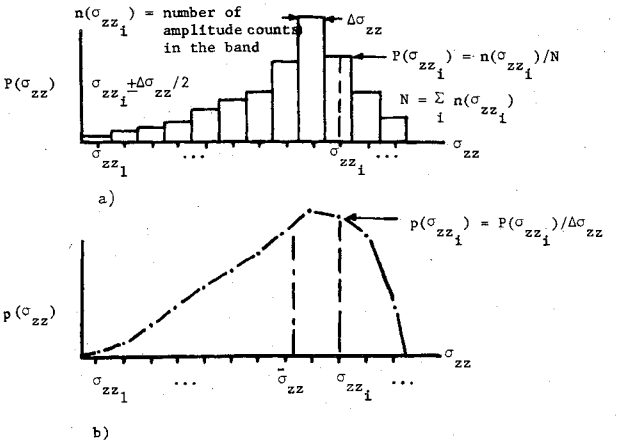


**Fig. 8 Amplitude distribution from frequency counts. a) Frequency distributions of $\sigma_{zz}$. b) Probability density function of $\sigma_{zz}$.**

any taxi speed $V_{\text{TAXI}}$. Since either $\sigma_{zz}(T_j)$ or $R_{zz_{T_j}}(0)$ is speed-independent, Eq. (11) may be written as

$$p_S(s, t) = p(\sigma_{zz}, \gamma, t) = p(\sigma_{zz}, t) p(\gamma, t)$$

Equation (12a) now becomes

$$E[S(T_j)] = \int_0^\infty \sigma_{zz}(T_j) p(\sigma_{zz}, T_j) d\sigma_{zz} \int_0^\infty e^{-\gamma |t-T_j|} p(\gamma, T_j) d\gamma$$

$$= \bar{\sigma}_{zz}(T_j) e^{-\bar{\gamma}_j |t-T_j|} \tag{12b}$$

The univariate density functions appearing in Eq. (12b) may be obtained by the classical frequency representation for the probability distribution at time $T_j$ from an ensemble of composite roughness records. A schematic diagram for evaluating $p(\sigma_{zz}, T_j)$ is shown in Fig. 7. It must be remembered that $\bar{\sigma}_{zz}(T_j)$ and $\bar{\gamma}_j$ of Eq. (12b) are merely the expected values of $\gamma_{zz}(T_j)$ and $\gamma(T_j)$, respectively. Their evaluations may be obtained, respectively, by the standard averaging procedure, i.e., by calculating the centroid of Fig. 8, and by using the moment-generating function[18] for the given probability density function $p(\gamma, T_j) = p(\gamma_j)$. Assuming $p(\gamma_j)$ is a Gaussian probability density function with mean $\bar{\gamma}_j$ and variance $\sigma_{\gamma_j}$, then it follows that

$$\int_{-\infty}^{\infty} e^{-\gamma_j |t-T_j|} p(\gamma_j) d\gamma_j$$

$$= \frac{1}{\sqrt{2\pi}\sigma_{\gamma_j}} \int_{-\infty}^{\infty} \exp\left[ -\gamma_j |t-T_j| - 1/2 \frac{(\gamma_j - \bar{\gamma}_j)^2}{\sigma_{\gamma_j}} \right] d\gamma_j$$

$$= e^{-\bar{\gamma}_j |t-T_j|} + \tfrac{1}{2}\sigma_{\gamma_j}^2 |t-T_j|^2 \simeq e^{-\bar{\gamma}_j |t-T_j|}$$

the approximation being valid for

$$\sigma_{\gamma_j}^2 << \bar{\gamma}_j \text{ or } |t-T_j|^2 \leq |t-T_j|.$$

## Generation of Nonstationary Composite Roughness Time History

Let $X(t)$ denote the sequence of random pulses that generates the expected composite roughness input, let $\bar{\sigma}_{zz}(T_j) = \bar{\sigma}_{zz_j}$ be the time dependent strength of the random pulses, and let

$$\int_0^\infty e^{-\gamma_j |t-T_j|} p(\gamma_j) d\gamma_j = e^{-\bar{\gamma}_\pi |t-T_j|}$$

be the deterministic shaping functions. Then the expected composite roughness input process may be represented in the form

$$X(t) = \sum_{j=1}^{N(t_{n+1})} \bar{\sigma}_{zz} e^{-\bar{\gamma}_j |t - T_j|} \tag{13}$$

where $N(t)$ is a general counting process, and $\bar{\sigma}_{zz_j}$ is purely random in the sense that $E[\bar{\sigma}_{zz_j}\bar{\sigma}_{zz_k}]E[\bar{\sigma}_{zz_j}]E[\bar{\rho}_{zz_k}]$, and $p(\bar{\sigma}_{zz,T_j}) = p(\bar{\sigma}_{zz})$ for $j=1,2,3,\ldots,n$ if $p(\bar{\sigma}_{zz})$ is obtainedin the following manner:

$$p(\bar{\sigma}_{zz}) = \lim_{\substack{t_{n+1}\to\infty \\ t\to 0}} \frac{1}{t_{n+1}-t_o} \int_{t_o}^{t_{n+1}} p(\bar{\sigma}_{zz}, t)\, dt \tag{14}$$

$$\approx \lim_{n\to\infty} \frac{1}{n} \sum_{j=1}^{n} p(\bar{\sigma}_{zz}, T_j)$$

It must be remembered that $X(t)$, the expected composite roughness input process, is defined in the interval $(t_o, t_{n+1})$ and may be represented by a single time history, such as Fig. 6 or the corresponding plot for the fleet fatigue evalution analysis. The latter was used in deriving Eq. (13). The extension to $X(t) = E[S(t)]$ is immediately obvious if one remembers the relation between $E[S^{(i)}(t)]$ and $E[S(t)]$ as expressed by the last equality in Eq. (9). Thus, the preliminary quantities are totally defined within the framework of available roughness data in power spectral density form and existing aircraft operational procedures with no sacrifice in mathematical rigor.

## Selection of Arrival Rate and Strength Distribution

A heuristic approach toward the understanding of the time averaging process on the time-dependent density functions as shown in Eq. (14) will prove that, for certain fleet operations, the time-independent strength density function analysis is more advantageous to use than the stringent time-dependent strength density functions analysis. Figure 7 illustrates the criteria for the choice of the most suitable combinations of arrival rate and strength distribution.

Case (a) is representative of the single record composite roughnesses for design criteria analysis. As a result of the two-time averaging [see Eqs. (9) and (10)], it is natural that the roughness strength be somewhat stabilized and the individual time-dependent strength density functions be close to that obtained from Eq. (14). The arrival rate will be more irregular because many aircraft of different types were involved. It is therefore reasonable to assume that an ergodic (stationary) strength distribution and nonhomogeneous Poisson arrival rate will suffice.

Case (b) is best demonstrated by the single record composite roughness for fatigue life evaluation based on fleet operations. The averaging is done over an ensemble of one type; hence, the different levels of the roughness strength are inherently present and sensitive to time in that the time-independent strength density function as derived from Eq. (14) will not be a representative strength density function at any given time. Due to the large number of aircraft in the ensemble, the arrival rates are quite irregular. Thus, the realistic choice of strength distribution and arrival rate will be nonstationary and nonhomogeneous Poisson, respectively.

Case (c) exemplifies the single time history of a given aircraft that performs prototype flight testing or a commercial airliner that flies scheduled revenue flights on predetermined routes. It is understood that such airplanes do have some built-in periodicity in the taxi sites and flying time. The levels of the roughness strength are selected, if not deterministic, and the arrival rates are correlated. A logical choice for the strength distribution and arrival rate for this case will be nonstationary and correlated.

## Power Spectral Densities of a Composite Roughness Record

The generalized power spectral density is defined as

$$\Phi_{XX}(\omega_1, \omega_2) = \frac{1}{(2\pi)^2} \int_{-\infty}^{\infty}\int_{-\infty}^{\infty} n_{xx}(t_1, t_2) e^{-j(\omega_1 t_1 - \omega_2 t_2)}\, dt_1 dt_2 \tag{15a}$$

(see Bendat, et al.,[19]) or

$$S_{XX}(\omega_1, \omega_2) = \frac{1}{(2\pi)^2} \int_{-\infty}^{\infty}\int_{-\infty}^{\infty} R_{xx}(t_1, t_2) e^{j(\omega_1 t_1 - \omega_2 t_2)}\, dt_1 dt_2 \tag{15b}$$

(see Roberts[20]) by different authors; and Eqs. (15a) and (15b) only differ in a sign reversal, and in the quantities (the covariance and the autocorrelation functions, respectively) to be transformed. $n_{xx}(t_1, t_2) = R_{xx}(t_1, t_2)$, if the means $n_x(t_1)$ and $n_x(t_2)$ vanish.

The generalized power spectral density for a composite roughness record $X(t)$ as shown in Eq. (13) may be obtained by using either Eq. (15a) or (15b) with the following mean and covariance function [21]

$$n_x(t) = \int_{t_o}^{t_{n+1}} \sum_{j=1}^{N(t_{n+1})} \delta(\tau - T_j)\bar{\sigma}_{zz}(\tau) w_j(t-\tau) g_1(\tau)\, d\tau$$

$$= \sum_{j=1}^{N(t_{n+1})} \bar{\sigma}_{zz}(T_j) w_j(t - T_j) g_1(T_j) \tag{16a}$$

$$n_{xx}(t_1, t_2) = \int_{t_o}^{t_{n+1}} \sum_{j=1}^{N(t_{n+1})} \delta(\tau - T_j)\bar{\sigma}_{zz}^2(\tau) w_j(t_1 - \tau)$$

$$\times w_j(t_2 - \tau) g_1(\tau)\, d\tau + \int_{t_o}^{(t_{n+1})} \sum_{j,k=1}^{N(t_{n+1})} \delta(\tau_1 - T_j)$$

$$\times \delta(\tau_2 - T_k)\bar{\sigma}_{zz}(\tau_1)\bar{\sigma}_{zz}(\tau_2)\, w_j(t_1 - \tau_1) w_k(t_2 - \tau_2)$$

$$\times g_2(\tau_1, \tau_2)\, d\tau_1 d\tau_2 = \sum_{j=1}^{N(t_{n+1})} \bar{\sigma}_{zz}^2(T_j) w_j(t_1 - T_j)$$

$$w_j(t_2 - T_j)\,[g_1(T_j)] \sum_{j,k=1}^{N(t_{n+1})} \bar{\sigma}_{zz}(T_j)\bar{\sigma}_{zz}(T_k)$$

$$w_j(t_1 - T_j) w_k(t_2 - T_k)\,[g_2(T_j, T_k)] \tag{16b}$$

where $\omega_j(t - T_j) = e^{-\bar{\gamma}_j |t - T_j|}$ and $g_1(\tau_1, \tau_2)$ and $g_2(\tau_1, \tau_2)$ are the first and second cumulant functions,[14] given in terms of the first two density functions by the relations $g_1(t) = f_1(t)$, $g_2(t_1, t_2) = f_2(t_1, t_2) - f_1(t_1) f_1(t_2)$. Substituting Eq. (16b) into Eq. (15a), the generalized power spectral density for a composite roughness record may be expressed as

$$\Phi_{XX}(\omega_1, \omega_2)$$

$$= \sum_{j=1}^{N(t_{n+1})} \bar{\sigma}^2_{zz}(T_j)\,[g_1(T_j) + g_2(T_j, T_j)]\, W_j(\omega_1) W_j^*(\omega_2)$$

$$+ \sum_{j\neq k=1}^{N(t_{n+1})} \bar{\sigma}_{zz}(T_j)\bar{\sigma}_{zz}(T_k)\,[g_2(T_j, T_k)]\, W_j(\omega_1) W_k^*(\omega_2) \tag{17a}$$

where the asterisk denotes the complex conjugate. The ordinary power spectral density is given by

$$\Phi_{XX}(\omega)=\Phi_{XX}(\omega,\omega)$$
$$=\sum_{j=1}^{N(t_{n+1})}\bar{\sigma}_{zz}^2(T_j)\,[g_1(T_j)+g_2(T_j,\,T_j)]\,|W_j(\omega)|^2$$
$$+\sum_{j\neq k=1}^{N(t_{n+1})}\bar{\sigma}_{zz}(T_j)\bar{\sigma}_{zz}(T_k)\,[g_2(T_j,\,T_k)]\,W_j(\omega)\,W_k^*(\omega) \tag{17b}$$

where $W_j(\omega_i)$ and $W_k(\omega_i)$, $i=1,\,2$ are the Fourier Transforms of the pulse shapes and are given by

$$W_k(\omega_i)=\frac{1}{2\pi}\int_{-\infty}^{\infty}w_k(t_i-T_k)\,e^{-j\omega_i(t_i-T_k)}\,d(t_i-T_k)$$

Using Eq. (15b) in place of Eq. (15a), the following expression is obtained:

$$S_{XX}(\omega_1,\,\omega_2)$$
$$=\sum_{j=1}^{N(t_{n+1})}\bar{\sigma}_{zz}^2(T_j)\{[g_1(T_j)+g_2(T_j,\,T_j)\,W_j^*(\omega_1)\,W_j(\omega_2)$$
$$+[g_1(T_j)\,W_j^*(\omega_1)]^2\delta(\omega_2)$$
$$+\sum_{j\neq k=1}^{N(t_{n+1})}\bar{\sigma}_{zz}(T_j)\bar{\sigma}_{zz}(T_k)\,[g_1(T_j)g_1(T_k)$$
$$+g_2(T_j,\,T_k)]\,W_j^*(\omega_1)\,W_k(\omega_2) \tag{18a}$$

and the ordinary power spectral density is given by

$$S_{XX}(\omega)=S_{XX}(\omega,\,\omega)$$
$$=\sum_{j=1}^{N(t_{n+1})}\bar{\sigma}_{zz}^2(T_j)\{[g_1(T_j)+g_2(T_j,\,T_j)]\,|W_j(\omega)|^2$$
$$+[g_1(T_j)\,W_j^*(\omega)]^2\delta(\omega)\}$$
$$+\sum_{j\neq k=1}^{N(t_{n+1})}\bar{\sigma}_{zz}(T_j)\bar{\sigma}_{zz}(T_k)\,[g_1(T_j)g_1(T_k)$$
$$+g_2(T_j,\,T_k)]\,W_j^*(\omega)\,W_k(\omega) \tag{18b}$$

Equations (17a–18b) show that a roughness input spectrum approach employing a narrow-band stationary Gaussian process yields an acceptable load exceedance curve expressed as[22]

$$M(y)=\sum_{j=1}^{n}\frac{t_j}{t_T}N_{oj}\exp\left[-y^2/\left(2\sigma_{yj}^2\frac{t_j}{t_T}\right)\right],\quad\sum_{j=1}^{n}t_j=t_T \tag{19}$$

where the $\sigma_{yj}$'s are obtained from one runway with $n$ discrete taxi speed segments at $t_j$ sec per segment, or given by Firebaugh[23] as

$$N(y)=\sum_{n=1}^{4}2N_oTP_ne^{-(y/sR_n)} \tag{20}$$

where $R_n=\sigma_y/\sigma_{h_n}$, with $\sigma_{h_n}$'s equal to 0.2 in., 0.28 in., 0.41 in., and 0.57 in. for $P_n$'s of 0.50, 0.32, 0.15, and 0.03, respectively. Equation (20) employs four types of roughnesses obtained empirically from 64 runways and 115 roughness power spectra. (Some of the runways are surveyed along the center line as well as lines parallel to the center line.) The reason behind this inadvertent agreement is that the term $[g_1(T_j)+g_2(T_j,\,T_j)]$ in the single summation of Eqs. (17a–18b) is usually much larger than the terms $[g_2(T_j,\,T_k)]$ or $[g_1(T_j)\cdot g_1(T_k)+g_2(T_j,\,T_k)]$ in the double summation of the respective equations if the $T_j$'s and $T_k$'s are not strongly correlated. This statement may be verified easily by assuming the arrival times are Poisson (see Eqs. (23a) and (23b). Then

$$[g_1(T_j)+g_2(T_j,\,T_j)]=g_1(T_j)=\lambda(T_j)$$
$$[g_2(T_j,\,T_k)]=0$$
$$[g_1(T_1)g_1(T_k)+g_2(T_j,\,T_k)]=\lambda(T_j)\lambda(T_k)$$

It is seen that $\lambda(T_j)\lambda(T_k)<<\lambda(T_j)$, for $\lambda(T_k)$ and $\lambda(T_j)<<1$ so that the double summation is negligible if the arrival times are uncorrelated or $T_j$ and $T_k$ are far apart. This indicates that approximations of the type expressed by Eqs. (19) and (20) are only valid for operations with mutually independent taxi events and the expressions from Eqs. (17a–18b) are the exact solutions with the interactions between different roughnesses included.

## Comparison of the Generalized Results

### Standard One-Runway, One-Constant-Speed Case

In view of the complexity of the mean and covariance functions as given by Eqs. (16a) and (16b), it is interesting to consider the limiting case where only one runway roughness is present. For this situation Eq. (13) reduces to

$$X(t)=\bar{\sigma}_{zz_1}w_1(t-T_1) \tag{21}$$

The analogous mean and covariance functions are obtained from Eqs. (16a) and (16b), respectively, by the following development:

$$m_X(t)=\int_{t_o}^{t_{n+1}}\bar{\sigma}_{XX}(\tau)\,w_1(t-\tau)\,g_1(\tau)\,\delta(\tau-T_1)\,d\tau$$
$$=\bar{\sigma}_{XX}(T_1)\,w_1(t-T_1)\,g_1(T_1) \tag{22a}$$

$$m_{XX}(t_1,t_2)=\int_{t_o}^{t_{n+1}}\bar{\sigma}_{XX}^2(\tau)\,w_1(t_1-\tau)\,w_1(t_2-\tau)\,g_1(\tau)\,\delta(\tau-T_1d\tau$$
$$=\int_{t_o}^{t_{n+1}}\int\bar{\sigma}_{XX}(\tau_1)\,\bar{\sigma}_{XX}(\tau_2)\,w_1(t_1-\tau_1)\,w_1(t_2-\tau_2)\,g_2(\tau_1,\,\tau_2)$$
$$\delta(\tau_1-T_1)\,\delta(\tau_2-T_1)\,d\tau_1d\tau_2\ddagger$$
$$=\bar{\sigma}_{XX}^2(T_1)\,w_1(t_1-T_1)\,w_1(t_2-T_1)\,[g_1(T_1)+g_2(T_1,\,T_1)] \tag{22b}$$

Because there is only one arrival at $T_1$, the counting process can be considered Poisson; hence

$$g_1(T_1)=f_1(T_1)=\lambda(T_1)=1 \tag{23a}$$
$$g_2(T_1,\,T_1)=f_2(T_1,\,T_1)-f_1^2(T_1)=f_1^2(T_1)-f_1^2(T_1)=0 \tag{23b}$$

‡The substitution of $w_2(t_2-\tau_2)=w_1(t_2-\tau_2)$ was used. Since $w_1(t_1-\tau_1)=e^{-\gamma_1|t_1-\tau_1|}=e^{-\alpha_1\beta_1/2|t_1-\tau_1|}$, and $w_2(t_2-\tau_2)=e^{-\gamma_2|t_2-\tau_2|}=e^{-\alpha_2\beta_1/2|t_2-\tau_2|}=w_1(t_2-\tau_2)$ still specify two different shaping functions, no inconsistency with Eq. (16b) has occurred. It is physically impossible to have a $w_2(t_2-\tau_2)=e^{-\alpha_2\beta_2/2|t_2-\tau_2|}$, as $\beta_1$ is the shaping factor of a single given runway (see Eq. (5).

Using Eqs. (23a) and (23b) in Eqs. (22a) and (22b), the mean and covariance functions of $X(t)$ are found to be

$$n_X(t) = \bar{\sigma}_{XX}(T_1)\, w_1(t-T_1) \tag{24a}$$

$$n_{XX}(t_1, t_2) = \bar{\sigma}^2_{XX}(T_1)\, w_1(t_1-T_1)\, w_1(t_2-T_1) \tag{24b}$$

From the shape of the shaping function, $w_1(t_1 - T_1) = e^{-\gamma_i |t_1 T_1|}$, $i=1,2$, it is apparent that Eq. (24b) is only meaningful when $|t_2 - t_1|$ is small or $t_2$ is close to $T_1$; otherwise, $w_1(t_2 - T_1)$ will approach zero and $n_{XX}(t_1, t_2)$ will vanish. To anticipate the fact that the autocorrelation function of $X(t)$ will resemble that of the standard one runway, one-constant taxi speed approach of Eqs. (4a) and (4b), it is necessary to show that $n_X(t) = \bar{\sigma}_{XX}(T_1)\, w_1(t-T_1) = 0$. This condition is readily satisfied for $|t - T_1| >> 0$. With the mean of $X(t) = 0$ established almost everywhere, remembering $|t_2 - t_1| \to \epsilon \to 0$, the autocorrelation function of $X(t)$ is

$$\begin{aligned}
\lim_{t_2 \to t_1} R_{XX}(t_1, t_2) &= \lim_{t_2 \to t_1} K_{XX}(t_1, t_2) \\
&= \lim_{t_2 \to t_1} [\bar{\sigma}^2_{XX}(T_1)\, W_1(t_1 - T_1)\, W_1(t_2 - T_1)] \\
&= \{\bar{\sigma}_{XX}(T_1)\, W_1(t_1 - T_1)\}^2 \\
&= \sigma^2_{XX}(T_1) e^{-\alpha_1 \beta_1 |t_1 - T_1|}
\end{aligned} \tag{25}$$

The last equality in Eq. (25) is exactly the same as Eq. (6), if one recognizes that $|t_1 - T_1| = |\tau|$. The subscript "1" merely indicates one runway ($\beta = \beta_1$), one speed ($\alpha = \alpha_1$), and one commencing time $T_1$.

The mean and covariance functions given by Eqs. (24a) and (24b) compare well with several published results. With obvious substitutions they agree with Lin's[15] results for a sequence of mutually independent, identically distributed strength pulses with either a nonhomogeneous Poisson arrival rate or correlated arrival times. They are the same as those given by Roberts[24] for the nonstationary Poisson distributed random pulses. Again with obvious substitutions they are the same as the corresponding equations given by Srinivasan, et al,[25] for a sequence of random pulses with nonstationary strength and correlated arrival rate.

## Generalized and Ordinary Output Power Spectral Densities

If the frequency response functions for the aircraft responses in question are furnished, their output power spectral densities may be calculated from the relations

$$\Phi_{YY}(\omega_1, \omega_2) = \Phi_{XX}(\omega_1, \omega_2) H(\omega_1) H^*(\omega_2) \tag{26a}$$

$$\Phi_{YY}(\omega) = \Omega_{XX}(\omega)\, |H(\omega)|^2 \tag{26b}$$

$S_{XX}(\omega_1, \omega_2)$ or $S_{XX}(\omega)$ may be used in lieu of $\Phi_{XX}(\omega_1, \omega_2)$ or $\Phi_{XX}(\omega)$ in Eqs. (26a) and (26b). However, for most response quantities, $H(0)H^*(0)$ and $|H(0)|^2$ are always zero and the evaluation of $\Phi_{YY}(0)$ or $\Phi_{YY}(0, 0)$ is not warranted. Nevertheless, the $S_{XX}(\omega_1, \omega_2)$ and $S_{XX}(\omega)$ will furnish comparatively more accurate response data for the outputs that are sensitive to very low frequencies (e.g., rigid body motions excited by long wavelength unevenness) and the selections of $\Phi_{XX}(\omega_1, \omega_1)$ and $\Phi_{XX}(\omega)$ may inadvertently introduce some unconservatism into the analysis. It is therefore advisable to calculate both $\Phi_{YY}(\omega_1, \omega_2)$ and $\Phi_{YY}(\omega)$ and $S_{YY}(\omega_1, \omega_2)$ and $S_{YY}(\omega)$.

## Conclusions

Same salient features that have not been revealed in the past are brought out through this general approach with considerably fewer restrictions. The main result for the composite roughness input spectrum is given by Eqs. (17a–18b). Also it is worth noting that the composite roughness spectra as represented by Eqs. (17a–18b) are the only exisiting analytical forms describing runway roughnesses by the variances ($\bar{\sigma}_{XX}$'s) of the constituent runways[23] as well as the only existing roughness representation including the interactions between runways (or bumps, etc.). Recalling that $w_j(t - T_j)$ is a given shaping function, then the procedure can easily be adapted to formulate the roughness of a deterministic runway, since it is always possible to match the profile by both bumps and dips of a known form, for example, $\sin[\pi(t - T_j)/a_j]$, $1 - \cos[\pi(t - T_j)/a_j]$, etc., with known strength $A_j$ at each uneven locality. The assessment of arrival times for the bumps and dips is inconsequential, since they are derived a priori from the known record in the form of time history $X(t)$ or a roughness profile, $X(x) = f(vt)$.

Finally, quantities appearing in Eqs. (17b) and (18b) are all available from the existing roughness power spectral densities or the given record. The method requires no additional profile measuring or data collecting on the roughnesses, although there might be some slight reprocessing of the power spectral densities in the event that the autocorrelation functions of the constituent roughnesses are not furnished together with the power spectral densities.

## References


[1] Liepmann, H. W., "On the Application of Statistical Concepts to the Buffeting Problem," *Journal of Aerospace Science*, Vol. 19, Dec., 1952, pp. 793–800.

[2] Press, H. and Mazelsky, B., "A Study of the Application of Power Spectral Methods of Generalized Harmonic Analysis to Gust Loads on Airplanes," NACA TN 2853, Jan. 1953.

[3] Fung, Y. C., "The Analysis of Dynamic Stresses in Aircraft Structures during Landing as Nonstationary Random Processes," *Journal of Applied Mechanics*, Vol. 22, Dec. 1955, pp. 449-457.

[4] Howell, L. J. and Lin, Y. K., "Response of Flight Vehicles to Nonstationary Atmospheric Turbulence," *AIAA Journal*, Vol. 9, Nov., 1971, pp. 2201–2207.

[5] Gaonkar, G. H. and Hohenemser, K. H., "Stochastic Properties of Turbulence Excited Rotor Blade Vibrations," *AIAA Journal*, Vol. 9, March 1971, pp. 419-424.

[6] Holman, R. E. and Hart, G., "Structural Response to Segmented Nonstationary Random Excitation," *AIAA Journal*, Vol. 10, Nov. 1972, pp. 1473–1478

[7] Walls, J.H., Houbolt, J.C., and Press, H., "Some Measurements of Power Spectra of Runway Roughness," NACA TN 3305, Jan. 1954.

[8] Houbolt, J. C. Walls, J. H., and Smiley, R. F., "On Spectral Analysis of Runway Roughness and Loads Developed During Taxiing," NACA TN 3484, July 1955.

[9] Morris, G. J., "Response of a Turbojet and a Piston-Engine Transport Airplane to Runway Roughness," NASA TN D-3161, Dec. 1965.

[10] Thompson, W. E., "Measurements and Power Spectra of Runway Roughness at Airports in Countries of the North Atlantic Treaty Organization," NACA TN 4303, July 1958.

[11] Morris, G. J. and Hall, A. W., "Recent Studies of Runway Roughness," NASA SP-83, May 1965, pp. 1-5.

[12] Tung, C. C., Penzien, J., and Horonjeff, R., "The Effect of Runway Unevenness on the Dynamic Response of Supersonic Transports," NASA CR-119, Oct. 1964.

[13] Hitch, H.P.Y., "The Behavior of Aircraft on Rudimentary Airstrips," *Proceedings of the Symposium on the Noise and Loading Actions of Helicopters, VSTOL Aircraft and Ground Effect Machines*, Sept. 1965, Institute of Sound and Vibration Research, University of Southampton, Great Britain.

[14] Lin, Y. K., "Application of Nonstationary Shot Noise in the Study of System Response to a Class of Nonstationary Excitations," *Journal of Applied Mechanics*, Series E, Vol. 30, Dec. 1963, pp. 555–558.

[15] Lin, Y. K., "Nonstationary Excitation and Response on Linear Systems Treated as Sequences of Random Pulses," *Journal of the Acoustical Society of America*, Vol. 38, March 1965, pp. 453–460.

[16] Houbolt, J. C.,"Interpretation and Design Application of Power Spectral Gust Response Analyses Result," *Proceedings of AIAA/ASME 7th Structures and Materials Conference*, Cocoa Beach, Fla., 1966, p. 83.

[17]Laning, J. H., Jr. and Battin, R. H., *Random Processes in Automatic Control,* McGraw-Hill, New York, 1956, pp. 63-65.

[18]Parzen, E., *Modern Probability Theory and Its Applications,* Wiley, New York, 1960, pp. 215-223.

[19]Bendat, J. S., Enochson, L. D., Klein, G. H., and Piersol, A. G., "Advanced Concepts of Stochastic Processes and Statistics for Flight Vehicle Vibration Estimation and Measurement," Aeronautical Systems Division, Wright-Patterson Air Force Base, Ohio, ASD-TDR-62-973, 1962, pp. 4-7.

[20]Roberts, J. B., "On the Harmonic Analysis of Evolutionary Random Vibration," *Journal of Sound Vibration,* Vol. 2, March, 1965, pp. 336-352

[21]Chen, R. P., "Generalized Power Spectral Density Analysis with Application to Aircraft Taxiing Problems," Thesis, School of Engineering Science and Mechanics, Georgia Institute of Technology, June 1969.

[22]Rich, M. J., Kenigsberg, I. J., Israel, M. H., and Cook, P. P., "Power Spectral Density Analysis of V/STOL Aircraft Structures," presented at the 24th Annual National Forum of the American Helicopter Society, May 1968.

[23]Firebaugh, J. M., "Estimation of Taxi Load Exceedances Using Power Spectral Methods," *Journal of Aircraft,* Vol. 5, Sept.-Oct. 1968, pp. 507-509.

[24]Roberts, J. B., "The Response of Linear Vibratory Systems to Random Impulses," *Journal of Sound Vibration,* April, 1965, pp. 375-390.

[25]Srinivasan, S. K., Subramanian, R., and Kumaraswampy, S., "Response of Linear Vibratory Systems to Nonstationary Stochastic Impulses," *Journal of Sound Vibration,* Vol. 6, Sept. 1967, pp. 169-179.

*From the AIAA Progress in Astronautics and Aeronautics Series*

**AERODYNAMICS OF BASE COMBUSTION—v. 40**

*Edited by S.N.B. Murthy and J.R. Osborn, Purdue University, A.W. Barrows and J.R. Ward, Ballistics Research Laboratories*

It is generally the objective of the designer of a moving vehicle to reduce the base drag—that is, to raise the base pressure to a value as close as possible to the freestream pressure. The most direct and obvious method of achieving this is to shape the body appropriately—for example, through boattailing or by introducing attachments. However, it is not feasible in all cases to make such geometrical changes, and then one may consider the possibility of injecting a fluid into the base region to raise the base pressure. This book is especially devoted to a study of the various aspects of base flow control through injection and combustion in the base region.

The determination of an optimal scheme of injection and combustion for reducing base drag requires an examination of the total flowfield, including the effects of Reynolds number and Mach number, and requires also a knowledge of the burning characteristics of the fuels that may be used for this purpose. The location of injection is also an important parameter, especially when there is combustion. There is engineering interest both in injection through the base and injection upstream of the base corner. Combustion upstream of the base corner is commonly referred to as external combustion. This book deals with both base and external combustion under small and large injection conditions.

The problem of base pressure control through the use of a properly placed combustion source requires background knowledge of both the fluid mechanics of wakes and base flows and the combustion characteristics of high-energy fuels such as powdered metals. The first paper in this volume is an extensive review of the fluid-mechanical literature on wakes and base flows, which may serve as a guide to the reader in his study of this aspect of the base pressure control problem.

*522 pp., 6x9, illus. $19.00 Mem. $35.00 List*

TO ORDER WRITE: Publications Dept., AIAA, 1290 Avenue of the Americas, New York, N.Y. 10019